

Content from this work may be used under the terms of the CC BY 3.0 licence (© 2018). Any distribution of this work must maintain attribution to the author(s), title of the work, publisher, and DOI.

# EARLY COMMISSIONING OF THE LUMINOSITY DITHER SYSTEM FOR SuperKEKB\*

M. Masuzawa<sup>†</sup>, Y. Funakoshi, T. Kawamoto, S. Nakamura, T. Oki, M. Tobiyama, S. Uehara, R. Ueki, KEK, 305-0801 Tsukuba, Japan  
A. S. Fisher, M.K. Sullivan, D. Brown, SLAC, 94025 Menlo Park, CA, USA  
U. Wienands, ANL 60439 Argonne, IL, USA  
P. Bambade, S. Di Carlo, D. Jehanno, C. Pang, LAL, 91898, Orsay, France  
D.El Khechen, CERN, 1211 Geneva, Switzerland

## Abstract

SuperKEKB is an electron–positron double ring collider that aims to achieve a peak luminosity of  $8 \times 10^{35} \text{ cm}^{-2}\text{s}^{-1}$  by using what is known as the “nano-beam” scheme. A luminosity dither system is employed for collision orbit feedback in the horizontal plane. This paper reports the dither hardware and algorithm tests during the SuperKEKB Phase II luminosity run.

## INTRODUCTION

The SuperKEKB collider [1] employs a luminosity dither system that is based on the collision feedback system previously used at SLAC for PEP-II [2, 3] for finding the horizontal offset at the interaction point (IP) that maximizes luminosity. The dithering feedback is different from that used for KEKB collision orbital feedback, where beam–beam deflection was used in both the vertical and horizontal planes. With the “nano-beam” scheme, the horizontal beam–beam parameters are much smaller than those at KEKB, and the detecting luminosity maximum orbit using beam–beam deflection is not as effective as KEKB. Therefore, a dithering method was introduced for SuperKEKB. A good collision condition is sought for by dithering the positron beam (LER), and once a good collision condition is found, it is maintained by an active orbital feedback, which moves the electron beam (HER) relative to the LER by creating a local bump at the IP. The dither system was tested with colliding beams for SuperKEKB Phase II commissioning.

## DITHERING SYSTEM

### Principle

When an LER beam is dithered sinusoidally in the horizontal plane, where the relative offset of the LER and HER are  $x_0$ , the variation in luminosity  $L$  is described as a function of the relative offset of the two beams  $x$ , as follows:

$$L(x) = L_0 \exp\left(-\frac{x^2}{2\Sigma_x^2}\right) \quad (1)$$

where

$$x = x_0 + \tilde{x} \cos \omega_x t \quad (2)$$

and

\*Work supported by U.S.-Japan Science and Technology Cooperation Program in High Energy Physics.

<sup>†</sup> mika.masuzawa@kek.jp

$$\Sigma_x^2 = \sigma_{x+}^{*eff2} + \sigma_{x-}^{*eff2} \quad (3)$$

The parameters  $\tilde{x}$ ,  $\omega_x$ ,  $\sigma_{x+}^{*eff}$ , and  $\sigma_{x-}^{*eff}$  represent the dithering amplitude, dithering frequency, effective horizontal LER, and HER beam size at the IP, respectively. The effective horizontal beam size is denoted as follows:

$$\sigma_{x\pm}^{*eff} = \sigma_z \sin \phi_c \quad (4)$$

where  $\phi_c$  and  $\sigma_z$  are the half crossing angles of the two beams at the IP and bunch length, respectively. Figure 1 shows a conceptual drawing of the colliding beams at SuperKEKB.

Expanding Eq. (1) for small offset  $x_0$  and dither amplitude  $\tilde{x}$ ,  $L$  can be rewritten as follows:

$$L(x) = L_0 \left( 1 - \frac{x_0 \tilde{x}}{\Sigma_x^2} \cos \omega_x t - \frac{\tilde{x}^2}{2\Sigma_x^2} \cos^2 \omega_x t \right) \exp\left(-\frac{x_0^2}{2\Sigma_x^2}\right) \quad (5)$$

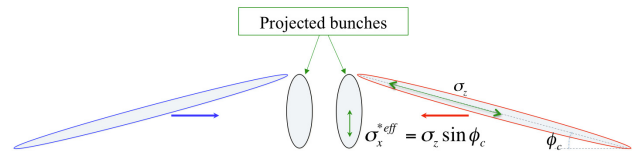


Figure 1: SuperKEKB colliding beams.

When the beam is dithered around the “center,” where luminosity peaks, luminosity drops on either side of the peak, giving a modulation at  $2\omega$ . When dithered off center, there is additional modulation at the fundamental, as indicated in Fig. 2.

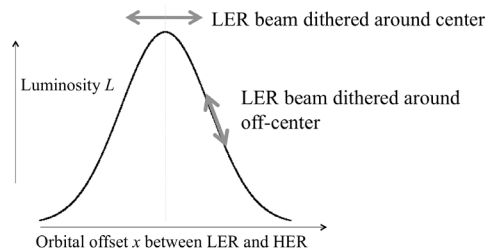


Figure 2: Luminosity dependence on the orbital offset between LER and HER at the IP.

In the dithering feedback loop, the offset between LER and HER at the IP is adjusted at each feedback cycle to minimize the amplitude of the fundamental harmonics in the luminosity signal. Twelve steering magnets in the HER, which are dedicated to orbital feedback, create a local bump at the IP to adjust the offset.

### Luminosity Monitors

Two types of fast luminosity monitors were used for studying dither in Phase II. They both detect photons, recoiled electrons, or positrons from radiative Bhabha scattering in the very forward (“zero degree”) direction. One monitoring system is called zero degree luminosity monitor (ZDLM) and is based on Cherenkov and scintillation counters [4]. The other system is developed by LAL, which uses diamond sensors and is called “LumiBelle2” [5]. The luminosity signals are input to the lock-in amplifier, which mixes them with the reference dither signal and then low-pass filtering to provide an output voltage proportional to  $L_0$  and  $x_0$  as follows:

$$V_x = CL_0 \frac{x_0 \tilde{x}}{\sqrt{2\Sigma_x^2}} \exp\left(-\frac{x_0^2}{2\Sigma_x^2}\right) \quad (6)$$

where  $C$  is the output conversion factor of the luminosity monitor.  $V_x$  is proportional to offset  $x_0$  and becomes zero when luminosity is maximized.

The feedback loop determines the amount and direction of offset correction. An algorithm based on Newton’s method with PI control was used for finding the zero of  $V_x$ .

### Dithering Hardware

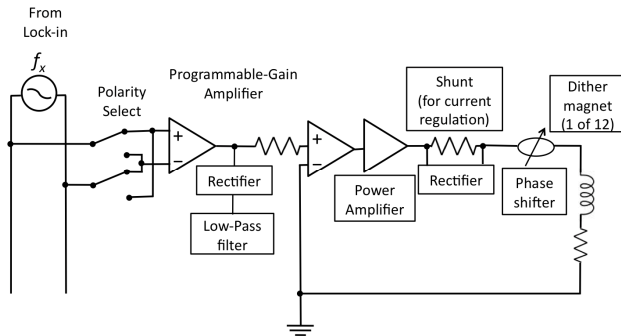


Figure 3: Dithering circuit.

A schematic diagram of the dithering system is shown in Fig. 3. A lock-in amplifier (AMETEK ADVANCED MEASUREMENT TECHNOLOGY model 7230) is used to generate a sine wave at a dither frequency. We chose 79 Hz as the dither frequency to avoid interference from the 50-Hz power line and injection frequencies of 1, 2, 5, 12.5, and 25 Hz. The sine wave is used as an input to the power supplies via a programmable-gain amplifier. There are 12 air-core Helmholtz coils installed in the LER to form a closed bump at the IP. The programmable-gain amplifier and coils were designed and fabricated by SLAC [6]. The

time delay was adjusted through the programmable amplifier by using the phase-shifter. The fudge factors of each coil were obtained by analyzing the actual beam orbit. They were used to improve the bump orbit during beam commissioning. The block diagram of the dither system is described elsewhere [7].

## COMMISSIONING

This section summarizes the results from the dithering study with colliding beams. The luminosity signals from ZDLM and LumiBelle2 were used as input to the lock-in amplifier. To maintain stable collision conditions, the collision feedback in the vertical direction (“iBump FB”) and continuous closed orbit correction (“CCC”), which keeps the global orbit in the entire ring to the reference orbit, were kept on. The HER and LER beam currents were kept as constant as possible by injecting the beam to both rings frequently. The current in the HER was varied from 235 mA to 250 mA, while it was varied from 285 mA to 300 mA in the LER. The LER beam was dithered at 79 Hz, with the dither amplitude being 20  $\mu\text{m}$  at the IP.

Four scanned data sets were taken using LumiBelle2 and ZDLM alternatively as input to the lock-in amplifier, with varying HER horizontal bump height at the IP, as shown in the example in Fig. 4. Table 1 summarises the scans.

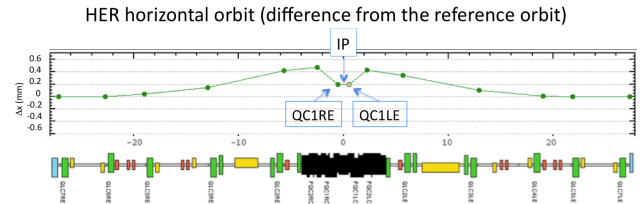


Figure 4: Local bump (0.2 mm as an example) at the IP in the HER is shown.

Table 1: Summary of Dither Study

	Input to lock-in amplifier	Scan range ( $\mu\text{m}$ )
Scan 1	LumiBelle2	-250 ~ +250
Scan 2	LumiBelle2	+250 ~ -250
Scan 3	ZDLM	-150 ~ +150
Scan 4	ZDLM	+150 ~ -150

### Luminosity Scan

Figure 5 shows the luminosity response when the bump height at the IP was changed during scan 3, as an example. The luminosity is normalized to its peak for each luminosity monitor. The normalized luminosity  $L_0$  is fitted by the following Gaussian functions:

$$L_0 = m_1 + \exp\left(-\frac{(x - m_2)^2}{2m_3^2}\right) \quad (7)$$

Content from this work may be used under the CC BY 3.0 licence (© 2018). Any distribution of this work must maintain attribution to the author(s), title of the work, publisher, and DOI.

where  $x$  is the beam position monitored by the beam position monitor (BPM) at a magnet called “QC1LE”. The fitted parameters  $m_2$  and  $m_3$  represent the HER beam position where the luminosity peaks and exhibits standard deviation, respectively.

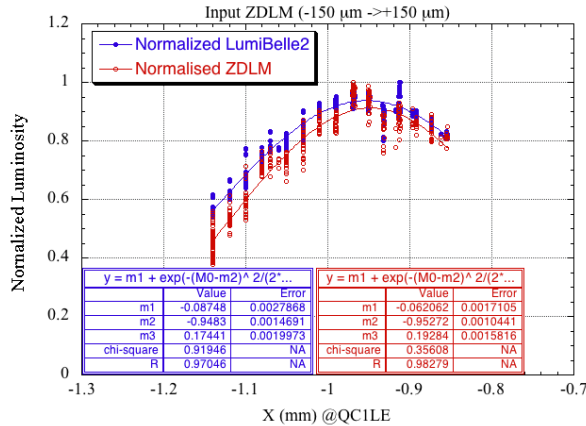


Figure 5: Luminosity is plotted against the beam position measured at the QC1LE BPM during scan 3.

Table 2 summarizes the fitted parameters. Luminosity peaks when the HER beam position measured at QC1LE is -0.95 mm for all scans, indicating that the effects of the bump magnet hysteresis and drift of the beam orbits are negligible.

Table 2: Summary of Gaussian-fitted Parameters

Detector	LumiBelle2		ZDLM	
	$m_2$	$m_3$	$m_2$	$m_3$
Scan 1	-0.94	0.27	-0.95	0.24
Scan 2	-0.94	0.21	-0.95	0.18
Scan 3	-0.95	0.17	-0.95	0.19
Scan 4	-0.94	0.20	-0.95	0.18

### Response of Lock-in Amplifier to Luminosity

The output voltage from the lock-in amplifier,  $V_x$  in Eq. (6) is plotted as a function of the horizontal beam position at QC1LE in Fig. 6 for scans 3 and 4, where the ZDLM signal was used as input to the lock-in amplifier. The output voltage becomes zero and the phase jump takes place at  $x = -0.95$  mm in both scans, which are consistent with the position of the luminosity peak.

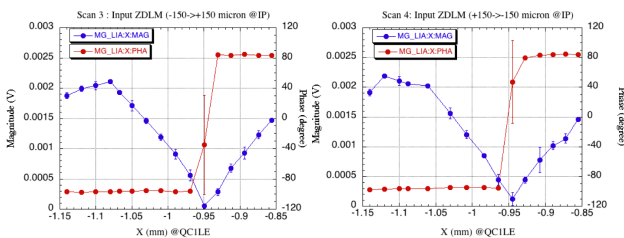


Figure 6:  $V_x$  (blue) and phase (red) are plotted against the HER beam position  $x$  for scans 3 (left) and 4 (right).

The plots of  $V_x$  and the phase for scans 1 and 2 are shown in Fig. 7, where LumiBelle2 was used as input to the lock-in amplifier. When  $V_x$  is zero, or close to zero, phase jump occurs. However, the beam position is not at  $x = -0.95$  mm but at  $x = -1.05$  mm. This does not match the beam position where luminosity peaks. The magnitude curve is not symmetric with respect to its minimum either, which is not the case with scans 3 and 4. The cause of this mismatch and asymmetric behavior will be investigated during Phase III that is scheduled to start in the spring of 2019.

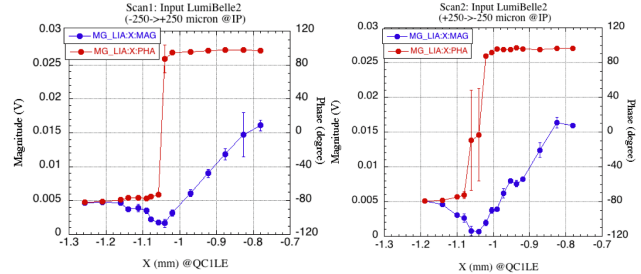


Figure 7:  $V_x$  (blue) and the phase (red) are plotted against the HER beam position  $x$  for scans 1 (left) and 2 (right).

### Dither Feedback

A feedback algorithm based on Newton’s method with PI control was first tested in May. The luminosity signal,  $V_x$ , and the bump height at the IP are plotted in Fig. 8.

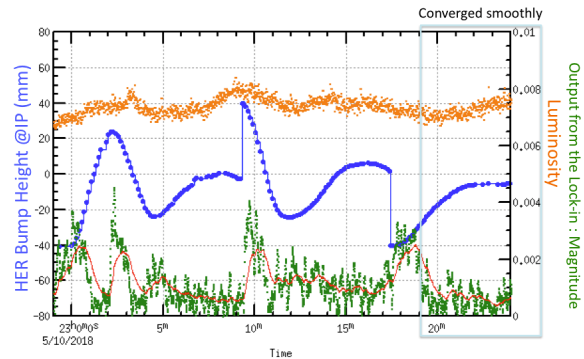


Figure 8:  $V_x$  (green) and bump height at the IP (blue) are plotted with luminosity (orange) during the dither feedback test.

The feedback algorithm loop runs in the main computer system. It determines a proper size and direction of the offset at the IP in the HER. These parameters are then sent to the magnet control system via EPICS to create a bump in the HER. The feedback loop set a bump in the correct direction and made the output from the lock-in amplifier smaller, though there were a couple of overshoots initially. After finding a good feedback parameter set, the feedback converged smoothly to an optimum value without any overshoot and  $V_x$  was brought to close to zero. The luminosity response was not clear this time, as the beam size was large and luminosity was low. Luminosity was not very sensitive to the horizontal beam offset in May.

The second feedback test was carried out in July when the beam size was smaller and luminosity was higher. We were expecting a clearer luminosity response to dither feedback but it turned out that it was not the case. This is probably because we used LumiBelle2 as input to the lock-in amplifier. LumiBelle2 seemed to have a problem when used as the input to the lock-in amplifier, as described earlier. Figure 9 shows  $V_x$  and the bump height that the dither feedback set. When the bump height was set to  $-40\ \mu\text{m}$ , the magnets reached the strength limit. An additional bump was created using different sets of steering magnets. When the feedback restarted,  $V_x$  continued to become smaller, though it did not stay at the minimum. An optimization of the feedback parameters in the PI control was needed, as the machine parameters were different. Though we did not have time to optimize the parameters, it is validated that the feedback algorithm can find the minimum  $V_x$  and the algorithm works in principle.

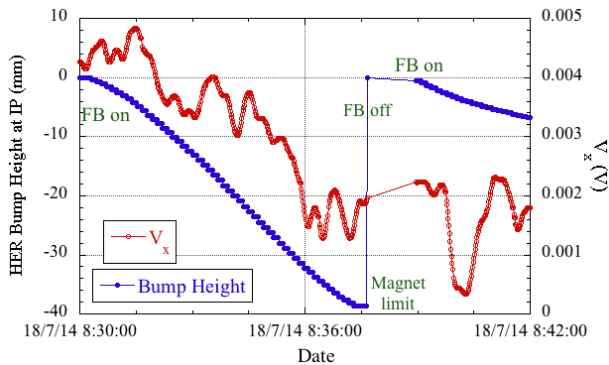


Figure 9:  $V_x$ , the bump height at the IP are plotted during the dither July feedback test.

### Response of Luminosity to Offset

Luminosity was fitted by Eq. (7) for the scans in the previous section. The bunch length was measured to be  $\sim 5.5\ \text{mm}$  for both LER and HER when the bunch current is  $\sim 0.3\ \text{mA}$  [8]. Using  $41.5\ \text{mrad}$  for  $\phi_c$  and  $5.5\ \text{mm}$  for  $\sigma_z$ , we obtain  $\sim 0.23\ \text{mm}$  for  $\sigma_{x\pm}^{\text{eff}}$  from Eq. (4). This is  $\sim 15\%$  larger than  $m_3$  in Table 2, except for scan 1. Luminosity degraded more than expected with a horizontal offset. This can be explained by considering the hourglass effect. When there is a crossing angle at the IP as is in SuperKEKB, a horizontal offset shift introduces a collision point shift in the beam direction, as is indicated in the left side drawing in Fig. 10. The vertical beta-function  $\beta_y$  is plotted on the right side. A  $100\text{-}\mu\text{m}$  horizontal offset makes  $\beta_y$  larger, which degrades luminosity by approximately  $10\%$  if  $\beta_y$  at the IP is  $3\ \text{mm}$ . If a horizontal offset causes beam blow-up at the IP, an additional degradation in luminosity will take place.

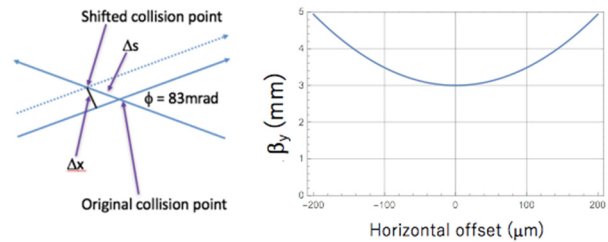


Figure 10: Hourglass effect when there is a horizontal offset at the IP.

## SUMMARY

The dither feedback system finds the optimum horizontal offset between the LER and HER to maximize luminosity by determining the minimum  $V_x$ . The optimum horizontal offset was found successfully when ZDLM was used as input to the lock-in amplifier. There was a shift of approximately  $100\ \mu\text{m}$  between the luminosity maximum offset and  $V_x$  minimum offset when LumiBelle2 was used as input. This will be investigated during the Phase III run.

The dependence of luminosity on offset agrees with the prediction estimated from the crossing angle, bunch length, horizontal beam size at the IP, and hourglass effect.

## REFERENCES

- [1] Y. Ohnishi *et al.*, “Report on SuperKEKB phase 2 commissioning”, in *Proc. IPAC’18*, Vancouver, BC, Canada, Apr.-May 2018, pp. 1-5. doi:10.18429/JACoW-IPAC2018-MOXGB1
- [2] S. Gierman *et al.*, “New fast dither system for PEP-II”, in *Proc. EPAC’06*, Edinburgh, UK, Jun. 2006, pp. 652-654.
- [3] A.S. Fisher *et al.*, “Commissioning the fast luminosity dither for PEP-II”, in *Proc. PAC’07*, Albuquerque, NM, USA, Jun. 2007, pp. 4165-4167. doi:10.1109/PAC.2007.4440072
- [4] T.Hirai, S. Uehara and Y.Watanabe, “Real-time luminosity monitor for B-factory experiment”, *Nuclear Instruments and Methods in Physics Research, Section A*, vol. 11, , pp. 670-676, Feb. 2001.
- [5] S. Di Carlo *et al.*, “Early Phase 2 Results of LumiBelle2 for the SuperKEKB Electron Ring”, in *Proc. IPAC’18*, Vancouver, BC, Canada, Apr.-May 2018, pp. 2934-2935. doi:10.18429/JACoW-IPAC2018-THYGBE4
- [6] U. Wienands *et al.*, “Dither coils for the SuperKEKB fast collision feedback system”, in *Proc. IPAC’15*, Richmond, VA, USA, May 2015, pp. 3500-3502. doi:10.18429/JACoW-IPAC2015-WEPWI006
- [7] Y. Funakoshi *et al.*, “Recent progress of dithering system at SuperKEKB”, in *Proc. IPAC’17*, Copenhagen, Denmark, May 2017, pp. 1827-1829. doi:10.18429/JACoW-IPAC2017-TUPIK059
- [8] H. Ikeda, private communication, Aug. 2018.